Orowan strengthening effect on the nanoindentation hardness of the ferrite matrix in microalloyed steels

Joonoh Moon [a], Sanghoon Kim [a], Jae-il Jang [a], Jongbong Lee [b], Changhee Lee [a],*

[a] *Division of Materials Science and Engineering, Hanyang University, 17 Haengdang-dong, Seongdong-ku, Seoul 133-791, Republic of Korea*
[b] *POSCO Technical Research Laboratory, 1, Geodong-dong, Nam-gu, Pohang, Gyeongbuk 790-785, Republic of Korea*

Abstract

Although it is well known that there is a significant contribution of precipitation strengthening to the strength of structural steels, it is difficult to experimentally separate the precipitation contribution from the overall strength due to the complex nature of steel microstructures. In this study, the contribution of precipitation strengthening to the matrix strength of ferrite in steel was experimentally investigated through nanoindentation tests. Nanoindentation hardness values of the ferrite matrix in precipitates-containing steels were greater than those in precipitate-free steels, which may be due to the Orowan strengthening mechanism based on the interaction between precipitates and dislocations. To better understand the precipitation strengthening contribution, interparticle spacing values of precipitates were calculated for each microalloyed steel and used for the analysis of hardness change. It was revealed that the trend of nanoindentation hardness change with variation in interparticle spacing corroborated the expectation based on classic Orowan theory.
© 2007 Published by Elsevier B.V.

1. Introduction

It has been well accepted that precipitation strengthening can significantly increase the matrix hardness of a metallic material [1]. Two major mechanisms have been suggested for explaining the precipitation strengthening, depending on the precipitates' penetrability to dislocation; particle shear mechanism (sometimes called cutting mechanism) for penetrable precipitates and Orowan mechanism for impenetrable ones [1], which are closely competing as main particle strengthening mechanism in a material including precipitates or dispersoids. Especially in microalloyed steel, there is little evidence of particle shear, and thus it is believed that precipitation strengthening is mainly controlled by Orowan mechanism, as reviewed in Ref. [1]. In Orowan mechanism [2], impenetrable precipitates in the matrix interrupt dislocation migration and thus plastic deformation via interaction with dislocations, which results in an increase in matrix strength. Most of the previous research [3–5] has measured the matrix strength from linear regression using the Hall–Petch relationship. Only a few studies have attempted to directly measure the matrix strength using nanoindentation test, which has made it possible to measure the mechanical properties on sub-micron size and thus individual phases in polycrystalline microstructure without the contribution of grain boundaries [6–10]. For example, Ohmura et al. [6] have shown that the matrix hardness of martensite (without the contributions of high angle grain boundaries, such as block, packet or prior austenite grain boundaries) increases with increasing carbon content.

In this work, the nanoindentation technique was adopted to experimentally verify the Orowan strengthening contribution to the matrix strength of ferrite in microalloyed steels. We observed that matrix hardness values of precipitate-containing steels are indeed greater than those of precipitate-free steels by precipitation strengthening. More interestingly, the change in nanoindentation hardness with interparticle spacing corroborated the expectation based on classic Orowan theory.

2. Experiments

The chemical compositions of the four steels examined in this study are listed in Table 1. Compared to steel A (which is a mild steel), steel B has more carbon content and steels C and

* Corresponding author. Tel.: +82 2 2220 0388; fax: +82 2 2293 4548.
E-mail address: chlee@hanyang.ac.kr (C. Lee).

Table 1
Chemical compositions of the tested steels (in wt%)

Alloy	C	Si	Mn	Ti	Nb	B (ppm)	N (ppm)
A	0.102	0.138	1.6	–	–	–	–
B	0.151	0.139	1.61	–	–	–	–
C	0.09	0.13	1.48	0.017	–	10	100
D	0.11	0.16	1.5	0.015	0.02	14	84

D additionally include microalloying elements, such as Ti and Nb, which are known to form precipitates. Note that steel D has both Ti and Nb while steel C has only Ti. Nanoindentation experiments were performed to a peak load of 10 mN at constant strain rate of $0.2\,\mathrm{s}^{-1}$ using Nanoindenter-XP (MTS Corp., Oak Ridge, TN) with a common Berkovich indenter. To observe the microstructure, the specimens were polished using conventional metallographic techniques and then slightly etched in a 3% Nital solution. The nanoindentation samples were electro-polished instead of mechanically polished to avoid surface hardening effect. Nanoindentation experiments were carefully performed in the center of a ferrite grain to avoid the grain boundary strengthening effect (see Fig. 1).

To observe precipitates, the specimens were etched in a mixed solution of methanol (80%) and perchloric acid (20%). A thin carbon film was deposited and extracted in the same etchant at a voltage of 2 V. The collected carbon replica was observed with a transmission electron microscopy (TEM, Model 2010, JEOL, Japan) and particles were identified by the selected area diffraction (SAD) pattern. The mean size of the distributed particles was measured by an image analyzer.
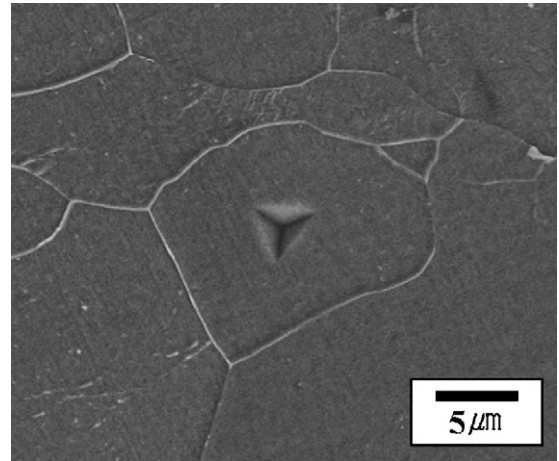

Fig. 1. Representative SEM image of hardness impression.

3. Results and discussion

3.1. Microstructure observation

Fig. 2 shows the microstructures of the four tested steels which consist of ferrite and a little pearlite. The ferrite grain size of steels C and D are smaller than those of steels A and B, which might be attributed to the grain growth inhibition by precipitates during alloy fabrication. The precipitate distribution in the matrix of steels C and D are shown in Fig. 3. From analysis using SAD pattern and energy dispersive spectroscopy (EDS), the precipitates in steels C and D were identified as TiN and (Ti, Nb)(C, N) respectively. Fig. 4 demonstrates the distribution in
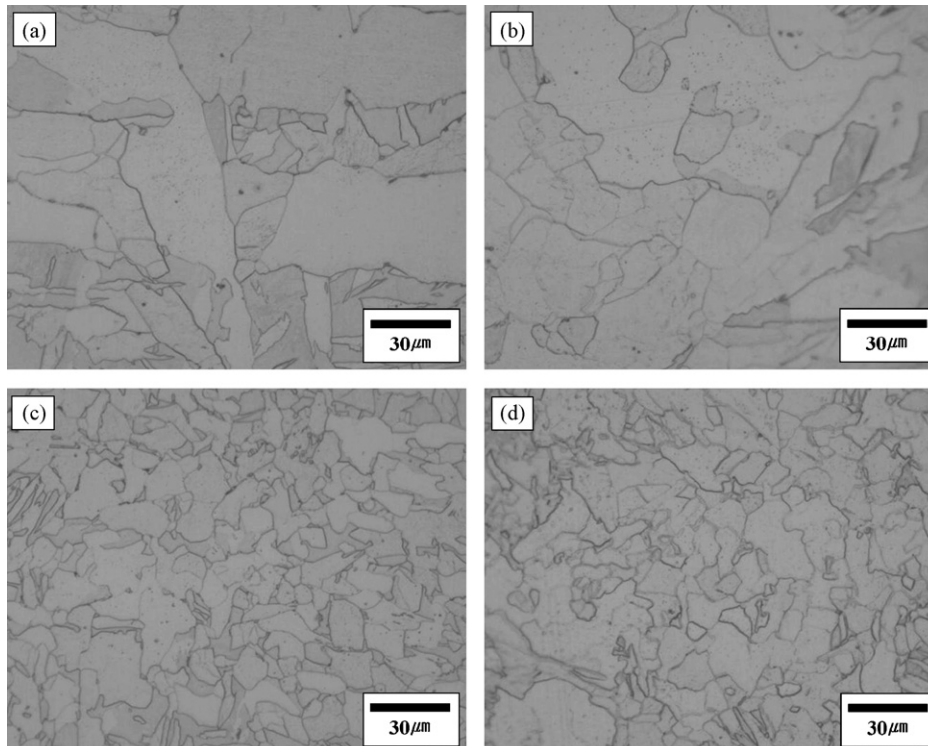

Fig. 2. Optical micrographs of (a) steel A, (b) steel B, (c) steel C and (d) steel D.
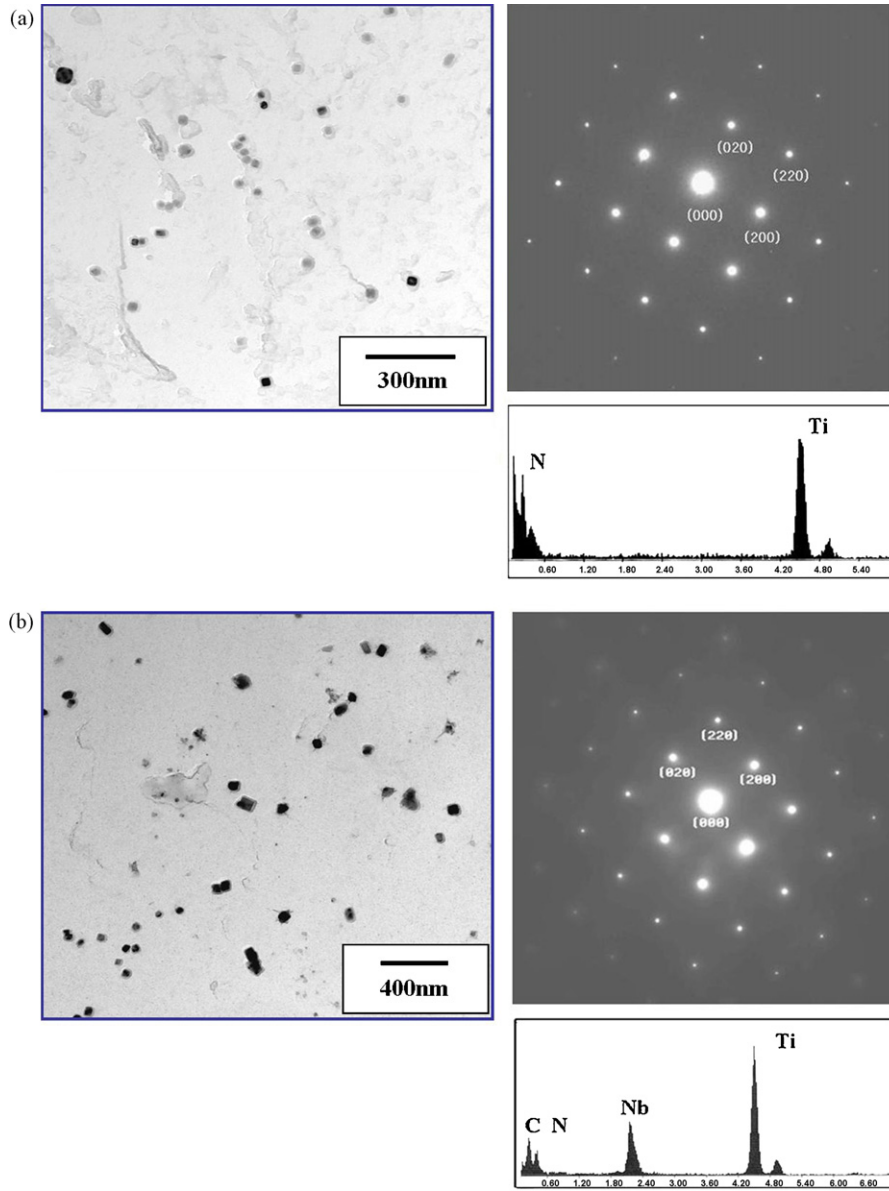
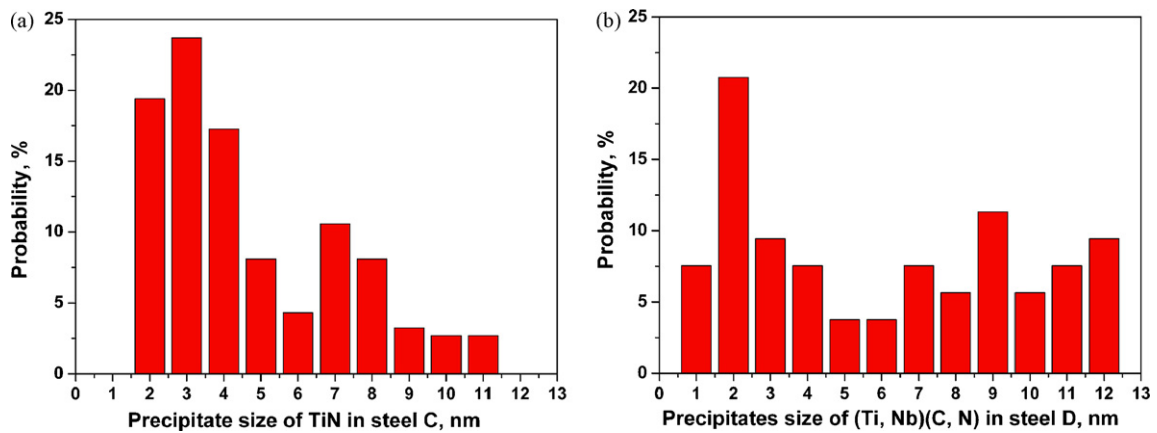Fig. 3. TEM images of (a) TiN precipitate in steel C and (b) (Ti, Nb)(C, N) complex precipitate in steel D.

Fig. 4. Size distribution of (a) TiN precipitate in steel C and (b) (Ti, Nb)(C, N) precipitates in steel D.
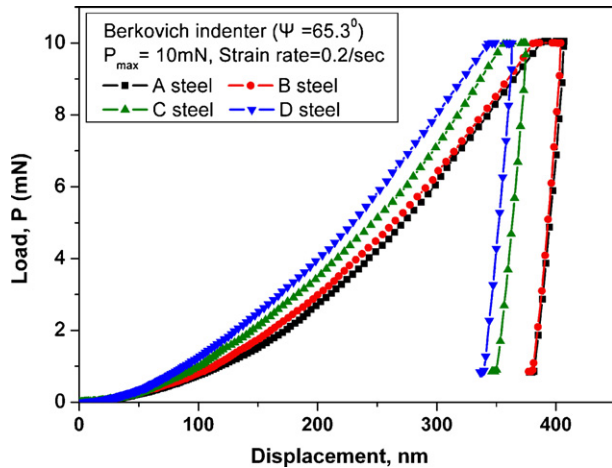
Fig. 5. Examples of *P–h* curves obtained by nanoindentation test of ferrite matrix.

the measured size of precipitates in steels C and D. While there was a large fluctuation in the size, mean sizes of TiN and (Ti, Nb)(C, N) were approximately 4 and 5 nm, respectively.

3.2. Nanoindentation

Fig. 5 shows a representative load–displacement curve of the steels recorded during nanoindentation test. The nanoindentation hardness values were calculated according to Oliver-Pharr method [11], and the results are summarized in Fig. 6. Note that the definition of nanoindentation hardness H (the peak load divided by the "projected area" of indentation A_P) is different from that of conventional macroscopic Vickers hardness HV (the peak load divided by the "surface area" of indentation A_S). The conversion from HV to H can be simply made as HV $= H \sin 68°$, which means that, in nature, the nanoindentation hardness should be higher than macroscopic HV. In Fig. 6, it is clearly seen that nanohardness values of steels C and D including precipitates were greater than those of steels A and B. The differences in hardness might be due to the effect of precipitation strengthening, as will be discussed below. Note that all the steels examined may have included Fe₃C precipi-
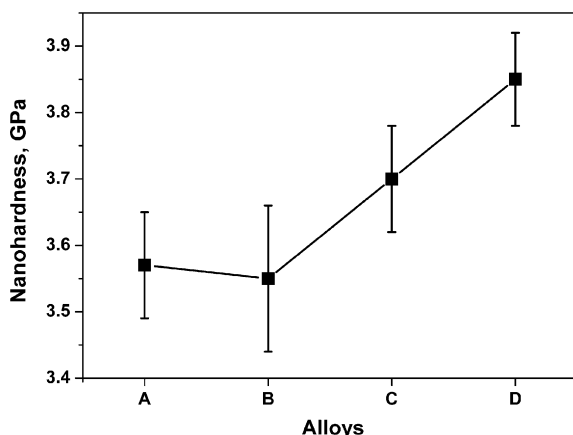
tates (cementite) without addition of microalloying elements, Nb and Ti. However, the cementite precipitates exist in pearlite lamellar phase consisting of ferrite and cementite, and the effect of cementite precipitate was neglected simply because only the matrix hardness of proeutectoid polygonal ferrite was measured.

On the other hand, even if steels A and B contain different carbon content (which can induce an interstitial solid-solution strengthening), nanohardness of these two alloys were nearly same. This similar nanohardness value may be explained by the high carbon contents of steels A and B, which was greater than the solubility limit, 0.02 wt% in ferrite matrix (see Table 1). Since additional carbon contents over solubility limit cannot affect the matrix strength, the solid solution contribution to the matrix strength in these two steels can be almost same.

3.3. Precipitation strengthening effect

As shown in Fig. 3, steels C and D contained a population of stabilized precipitates, which were due to microalloying elements such as Ti and Nb, and thus their matrix hardness values were greater than those of steels A and B possibly due to precipitation strengthening. As mentioned earlier, although cutting mechanism and Orowan mechanism are typically competing in a material having precipitates, it is believed that precipitation strengthening in microalloyed steels is mainly controlled by Orowan mechanism [1]. This is simply because the precipitates, such as nitrides and carbonitrides observed in this work, are too hard to be cut by dislocations. While one might expect that dislocations may be able to cut them when precipitates are extremely small, France et al. [12] reported that Orowan mechanism is still available in the case of the steels with nanometric precipitates (whose radii are about 1.5 nm which is smaller than those in this work). Accordingly, here we considered the Orowan mechanism as the main precipitate strengthening mechanism in the steels C and D.

Separation of the precipitation strengthening contribution from overall strength can be made by a simple analysis as follows. By combining the well-known Hall–Petch equation [13,14] and Tabor's empirical relationship $H \approx 3\sigma$ [15], the following equation was obtained;

$$H = H_0 + k_H d^{-1/2} \tag{1}$$

where H is the overall hardness of the tested material, H_0 is the matrix hardness and k_H is a modified locking parameter. As suggested by many researchers (for example, see Ref. [16]), the matrix hardness can be further divided again into more detailed terms based on different sources of the strengthening mechanism;

$$H_0 = H_0^* + H_{SS} + H_{Oro} \tag{2}$$

where H_0^* is the inherent hardness of the ferrite matrix itself without the effect of solute atoms and precipitates, H_{SS} is the solid-solution strengthening contribution and H_{Oro} is the precipitate strengthening contribution.

Fig. 6. Nanohardness of ferrite matrix measured by the nanoindentation test.
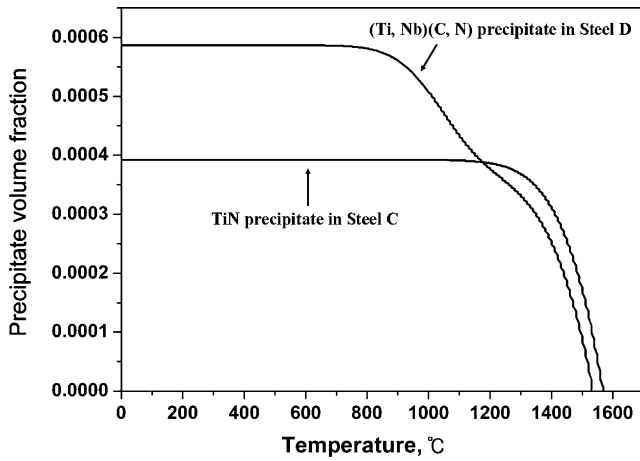
Fig. 7. Equilibrium precipitate volume fraction of TiN and (Ti, Nb)(C, N) in steels C and D.

Generally, the strength increase by Orowan mechanism can be expressed as [2]

$$\tau_{Oro} = \frac{Gb}{\lambda}, \tag{3}$$

where G and b are shear modulus of matrix and Burgers vector, respectively. The parameter λ in the equation is the interparticle spacing between dispersoids which is given as [3]

$$\lambda = \frac{4(1-f)r}{3f} \tag{4}$$

where f is the precipitate volume fraction and r is the precipitate size. Therefore, by applying Tabor's relationship [8] and Von Mises flow rule, $\tau = \sigma_y/\sqrt{3}$, Eq. (3) can be rewritten as

$$H_{Oro} = 3\sigma_{Oro} = 3\sqrt{3}\tau_{Oro} = \frac{3\sqrt{3}Gb}{\lambda}. \tag{5}$$

In this study, the interparticle spacing from Eq. (4) was calculated using both the precipitate size measured from the TEM micrographs (Figs. 3 and 4) and particle volume fraction calculated by the Thermo-clac (Fig. 7). As summarized in Table 2, the mean interparticle spacing of steel D (11.5 μm) was much smaller than that of steel C (14.03 μm). Thus, one might expect through Eq. (5) that nanoindentation hardness of matrix in steel D is greater than that in steel C if shear modulus (G) and Burgers vector (b) in the equation did not significantly vary. This expectation corroborated the qualitative trend of hardness change shown in Fig. 6. With taking this into consideration, it is believed that the classic equation for Orowan strengthening effect (i.e., Eq. (3)) is indeed valid and can be useful for explaining the contribution of precipitation strengthening to the overall strength.

Before closing, it is constructive to note that the increase in the nanoindentation hardness thanks to the precipitate strengthening is not exactly matched with that expected based on the change in the interparticle spacing according to Eq. (5); i.e., the difference in the mean interparticle spacing between steels C (11.5 μm) and D (14.03 μm) is about 20% while the difference in increasing amount of hardness (compared with those of steels B and C) between steels C (0.15 GPa) and D (0.3 GPa) is about twice. This uncertainty might arise from the nature of the precipitates as well as characteristics of nanoindentation experiments; first, the size of the particles shows a significant fluctuation, which results in a large fluctuation in interparticle spacing. This makes it hard to quantitatively judge the strengthening effects; second, since the particles are not uniformly distributed within a grain while nanoindentation is made in very small volume, the local interparticle spacing of the precipitates included in the plastic zone produced during indentation is conceivably varying significantly, which results in a large scatter in hardness value (see Fig. 6) and makes a quantitative evaluation difficult too; finally, the well-known 'indentation size effect (ISE)' (i.e., indentation hardness increases with decreasing indentation depth) might bring some uncertainty, as it is not clear that quantitative amount of ISE is the same for all steels examined here.

4. Conclusions

In the present paper, we report somewhat new experimental verification of precipitation strengthening contribution to the matrix strength in microalloyed steels. Nanoindentation results indicated that the hardness values of precipitate-containing microalloyed steels were much greater than those of precipitate-free steels. Additionally, interparticle spacing values of precipitates in the microalloyed steels were calculated to better understand the precipitation strengthening contribution. Indeed, the trend of nanoindentation hardness change with interparticle spacing is well matched with the expectation based on classic Orowan theory.

References

[1] M.A. Meyers, K.K. Chawla, Mechanical Behavior of Materials, Prentice Hall Inc., New Jersey, 1999, pp. 484, 491.
[2] E. Orowan, Symposium on International Stresses, Inst. of Metal, London, 1947, p. 451.
[3] M.Y. Liu, B. Shi, C. Wang, S.K. Ji, X. Cai, H.W. Song, Mater. Lett. 57 (2003) 2798.
[4] H. Hitaka, T. Tsuchiyama, S. Takaki, Scripta Mater. 44 (2001) 1503.
[5] M.-C. Zhao, T. Hanamura, H. Qiu, K. Nagai, K. Yang, Scripta Mater. 54 (2006) 1193.
[6] T. Ohmura, K. Tsuzaki, S. Matsuoka, Scripta Mater. 45 (2001) 889.
[7] Y. Choi, W.Y. Choo, D. Kwon, Scripta Mater. 45 (2001) 1401.

Table 2
Mean precipitate size, precipitate volume fraction and interparticle spacing

Alloy	Mean precipitate size (nm)	Precipitate volume fraction	Interparticle spacing (λ) (μm)
C	4 ± 2.4	3.8×10^{-4}	14.03 ± 8.42
D	5 ± 2.4	5.8×10^{-4}	11.5 ± 8.27

[8] Q. Furnemont, M. Kempf, P.J. Jacques, M. Göken, F. Delannay, Mater. Sci. Eng. A328 (2002) 26.

[9] M. Delince, P.J. Jacques, T. Pardoen, Acta Mater. 54 (2006) 3395.

[10] J.-I. Jang, S. Shim, S. Komazaki, T. Honda, J. Mater. Res. 22 (2007) 175.

[11] W.C. Oliver, G.M. Pharr, J. Mater. Res. 7 (1992) 1564.

[12] C. France, H. Klocker, J. Le Coze, A. Fraczkiewicz, Acta Mater. 45 (1997) 2789.

[13] E.O. Hall, Proc. Phys. Soc. Lond. 643 (1951) 747.

[14] N.J. Petch, J. Iron Steel Inst. 174 (1953) 25.

[15] M.F. Ashby, D.R.H. Jones, Engineering Materials, vol. 1, Pergamon Press, Oxford, 1980, p. 105.

[16] D. Srinivasan, R. Corderman, P.R. Subramanian, Mater. Sci. Eng. A 416 (2006) 211.